Environmental Toxicology and Pharmacology 108 (2024) 104453

Contents lists available at ScienceDirect

Environmental Toxicology and Pharmacology

journal homepage: www.elsevier.com/locate/etap

Antagonistic effects of a COX1/2 inhibitor drug in human HepG2 cells exposed to an environmental carcinogen

Carla Martins [a,b,c,*], Marcos Felipe de Oliveira Galvão [c], Pedro M. Costa [a,b], Kristian Dreij [c,**]

[a] Associate Laboratory i4HB Institute for Health and Bioeconomy, NOVA School of Science and Technology, NOVA University of Lisbon, Caparica 2819 516, Portugal
[b] UCIBIO Applied Molecular Biosciences Unit, Department of Life Sciences, NOVA School of Science and Technology, NOVA University of Lisbon, Caparica 2819 516, Portugal
[c] Unit of Biochemical Toxicology, Institute of Environmental Medicine, Karolinska Institutet, Box 210, Stockholm SE-171 77, Sweden

ARTICLE INFO

Edited by Malcolm D. Tingle

Keywords:
Benzo[*a*]pyrene
Diclofenac
Mixtures
In vitro
Genotoxicity
CYP1

ABSTRACT

Understanding interactions between legacy and emerging environmental contaminants has important implications for risk assessment, especially when mutagens and carcinogens are involved, whose critical effects are chronic and therefore difficult to predict. The current work aimed to investigate potential interactions between benzo[*a*]pyrene (B[*a*]P), a carcinogenic polycyclic aromatic hydrocarbon and legacy pollutant, and diclofenac (DFC), a non-steroidal anti-inflammatory drug and pollutant of emerging concern, and how DFC affects B[*a*]P toxicity. Exposure to binary mixtures of these chemicals resulted in substantially reduced cytotoxicity in human HepG2 cells compared to single-chemical exposures. Significant antagonistic effects were observed in response to high concentrations of B[*a*]P in combination with DFC at IC_{50} and ⅓ IC_{50}. While additive effects were found for levels of intracellular reactive oxygen species, antagonistic mixture effects were observed for genotoxicity. B[*a*]P induced DNA strand breaks, γH2AX activation, and micronuclei formation at ½ IC_{50} concentrations or lower, whereas DFC induced only low levels of DNA strand breaks. Their mixture caused significantly lower levels of genotoxicity by all three endpoints compared to those expected based on concentration additivity. In addition, antagonistic mixture effects on CYP1 enzyme activity suggested that the observed reduced genotoxicity of B[*a*]P was due to its reduced metabolic activation as a result of enzymatic inhibition by DFC. Overall, the findings further support the growing concern that co-exposure to environmental toxicants and their non-additive interactions may be a confounding factor that should not be neglected in environmental and human health risk assessment.

1. Introduction

The advancing human society is releasing increasing amounts and diversity of domestic, urban, industrial, and agricultural toxicants to the environment, with serious implications for both wildlife and human health (Bernanke and Köhler, 2009; Pereira et al., 2015). As a result, the environment is contaminated by increasingly complex mixtures of legacy ('traditional') and emerging ('novel') pollutants. It is critical to address effects of mixtures to establish more realistic monitoring policies and guidelines for risk assessment toward environmental and human health (Beronius et al., 2020; Martin et al., 2021; Silins and Högberg, 2011). The hazard and risk assessment of mixtures is based upon the concepts of additivity and interaction in accordance with the individual chemicals' mode-of-action (Cassee et al., 1998). Interaction effects can be categorized as antagonistic or synergistic (Hernández et al., 2017) producing unexpected outcomes and pose a serious confounding factor in the field of toxicology. Most notably, interaction effects constitute a further challenge since they depend not only on the compounds' mode-of-actions but also on the number of contaminants in the mixture, the concentration range of each chemical and their ratios (Altenburger et al., 2012; Ferreira et al., 2008; Nys et al., 2015).

The potential problem of toxicant interactions was further exacerbated by the end of 20th century, when it became clear that the exponential use of pharmaceutical drugs created another generation of

* Corresponding author at: Associate Laboratory i4HB Institute for Health and Bioeconomy, NOVA School of Science and Technology, NOVA University of Lisbon, Caparica 2819 516, Portugal.
** Corresponding author.
E-mail addresses: c.martins@campus.fct.unl.pt (C. Martins), kristian.dreij@ki.se (K. Dreij).

https://doi.org/10.1016/j.etap.2024.104453
Received 23 January 2024; Accepted 17 April 2024
Available online 18 April 2024
1382-6689/© 2024 The Authors. Published by Elsevier B.V. This is an open access article under the CC BY license (http://creativecommons.org/licenses/by/4.0/).

pollutants of emerging concern (Escher et al., 2011; Ternes, 1998). These emerging pollutants (and their derivatives) have turned into significant pollutants of surface waters in both developed and developing countries, either due to inefficient or absence of wastewater treatment and proper environmental guidelines (Rehman et al., 2015; Selwe et al., 2022; Verlicchi et al., 2012). In turn, legacy pollutants have been and are still the cause of high incidences of both acute and chronic health effects (WHO, 2021). The interaction between emerging and legacy pollutants is a realistic issue and a serious challenge for both ecosystems and human health. For example, numerous metabolic changes were observed in *Daphnia magna* exposed to a mixture of the emerging pollutant carbamazepine and perfluorooctane sulfonic acid, a representative of legacy pollutants, compared to single exposures (Wagner et al., 2018). This issue is especially relevant since pharmaceuticals such as non-steroidal anti-inflammatory drugs (NSAIDs) that inhibit cyclooxygenases (COX) and legacy pollutants can affect the same pathophysiological pathways, such as those related to inflammation and cancer. Indeed, it is suspected that cancer induced by environmental factors, especially chemicals, represent most of the cases (see for instance the reviews Lewandowska et al., 2019; Wogan et al., 2004).

The human PAH carcinogen benzo[*a*]pyrene (B[*a*]P) is a well-established model compound for legacy pollutants. The main emission sources for PAHs are wide, from incomplete combustion of petrogenic and biomass fuels to cigarette smoke and industrial waste (Boström et al., 2002). B[*a*]P is genotoxic and mutagenic, forming bulky DNA adducts after bioactivation by CYP1A1 and 1B1 into highly reactive B[*a*]P diol epoxides (Shimada and Fujii-Kuriyama, 2004). These adducts can hinder DNA replication and transcription; however, their removal can be cumbersome and result in DNA double strand breaks and subsequent formation of micronucleus (MN) (Harding et al., 2017; Shah et al., 2016). Most importantly, these lesions are known to cause so-called "hotspot" mutations in *ras* family oncogenes (activating transcription) and *p53* tumour suppressor gene (inhibiting function), which promotes cell proliferation and inhibition of apoptosis, both of which are hallmarks of neoplasia (Denissenko et al., 1996; Ross and Nesnow, 1999). Additionally, quinones formed by aldo-keto reductases (AKRs) can increase ROS formation and oxidative DNA damage (Penning, 2014). Consequently, the increased secretion of pro-inflammatory cytokines induced by oxidative stress resulting from B[*a*]P bioactivation may further promote cell proliferation which is a strong indicator of its potency as a complete carcinogen (Nebert et al., 2000; Shimada, 2006).

In turn, diclofenac (DFC) is a drug widely used in humans and livestock, generally considered safe albeit highlighted as one of the most toxic NSAIDs to some domestic animals and wildlife (Oaks et al., 2004). DFC was included on the "Watch List of EU Decision 2015/495" to increase the knowledge about its toxicity and mode-of-action. Although no longer on this list, DFC is still considered a "contaminant of emerging concern" (Khan et al., 2022; Sathishkumar et al., 2020; Yu et al., 2024). DFC exerts is pharmacological activity by inhibiting COX-1 and COX-2, i.e., prostaglandin synthases (Gan, 2010). Metabolization by cytochrome P450 (mainly CYP2C9 and CYP3A4) during phase I and by UDP-glucuronosyltransferases during phase II (see for instance the review Boelsterli, 2003) produces some metabolites that are associated with hepatotoxicity and hypersensitivity (Inoue et al., 2020). These effects are mainly associated with the induction of intracellular reactive oxygen species (ROS), which can influence mitochondrial integrity allied with suppression of autophagy (Jung et al., 2020) and induction of intrinsic apoptosis through caspases 9 and 3 (Inoue et al., 2004). In contrast to B[*a*]P, DFC has not been found to have genotoxic and carcinogenic potential *in vivo* or *in vitro* (Hartmann et al., 2021). In fact, as noted for other NSAIDs, it is suggested that DFC can hold some anti-cancer properties by inhibiting angiogenesis and cytokine signalling (Arisan et al., 2018; Duval et al., 2019; Kaur and Sanyal, 2011).

In Europe, B[*a*]P and DFC concentrations in surface waters have been found to exceed environmental quality standards (B[*a*]P: 1.7×10^{-4} μg/L and DFC: 0.1 μg/L), although with a decreasing trend (Škrbić et al., 2018; Vystavna et al., 2018). This makes them relevant model toxicants to study possible mixture interactions between legacy and emerging pollutants. Thus, the main objective of this study was to infer how DFC affects the toxicity of B[*a*]P. To accomplish this, we exposed hepatoma derived HepG2 cells to single compounds and binary mixtures of B[*a*]P and DFC. HepG2 cells were chosen as *in vitro* model due to their high metabolic capacity (Knasmüller et al., 1998). Considering the toxic properties of B[*a*]P, the scope of the current work centered on endpoints related to cytotoxicity, oxidative stress, genotoxicity, and impact on CYP1 enzyme activation.

2. Methods

2.1. Chemicals and cell culture

Benzo[*a*]pyrene (B[*a*]P) (CAS 50–32–8, > 95.0 %) was purchased from TCI EUROPE (Zwijndrecht, Belgium) and sodium diclofenac (DFC) (CAS 15307–79–6, 98 %) from Acros organics (Geel, Belgium). Stock solutions of B[*a*]P and DFC were prepared in dimethyl sulfoxide (DMSO, 99 %) from Sigma Aldrich (St. Louis, MO). The human hepatocellular carcinoma HepG2 cell line was acquired from the American Type Culture Collection (Rockville, MD). Cells were cultured in Corning® T-75 flasks with 10 mL of Minimum Essential Medium (MEM) supplemented with penicillin-streptomycin (100 IU/mL penicillin and 100 μg/mL streptomycin), 10 % v/v foetal bovine serum, sodium pyruvate (1 mM) and non-essential amino acid solution (0.1 mM), all purchased from Gibco by Life Technologies (Stockholm, Sweden). Cells were kept in an incubator, with humified atmosphere at 5 % CO_2 and 37 °C to maintain the proper cell growth during culture and assays. Cells were exposed, in fresh DMEM medium, to solvent control (0.1 % DMSO), B[*a*]P (3.2×10^{-3} to 10 μM), DFC (3.2×10^{-3} to 10^3 μM)or three different binary mixtures of B[*a*]P and DFC (Mixture 1: ⅕ IC_{50} of both, Mixture 2: ½ IC_{50} of B[*a*]P and ⅕ IC_{50} of DFC, Mixture 3: ½ IC_{50} of B[*a*]P and ½ IC_{50} of DFC), respectively for up to 48 h.

2.2. Cell viability assay

The impact on cell viability was determined using Alamar Blue (Invitrogen, Carlsbad, CA) after 48 h of exposure (Rampersad, 2012). This assay was used to determine half-maximal inhibitory concentrations (IC_{50}) of B[*a*]P and DFC. Subsequently, cells were exposed to IC_{50} and ⅕ IC_{50} concentrations of either compound mixed with the full range of concentrations of the other. Cells were seeded (1.5×10^4 cells/mL) in 96-well plates 24 h before exposure. After exposure, 20 μL of Alamar Blue was added to each well and the cells incubated for further 2 h. Fluorescence intensity (excitation 540 nm, emission 590 nm) was recorded using a microplate reader (Infinite F 200 PRO, fitted with the software: Magellan 7.2, all from Tecan, Austria). Every exposure was performed in triplicate technical replicates per plate, with four independent experimental replicates ($n = 4$).

2.3. Reactive oxygen species assay

The quantification of intracellular reactive oxygen species (ROS) was performed using the dichloro-fluorescein diacetate (DCFH-DA) assay (Wang and Joseph, 1999). In brief, cells were seeded in black 96-well plates with clear bottom (Corning Incorporated, NY) at 2.5×10^5 cells/mL 24 h before exposure. Cells were exposed for up to 12 h and using 1 mM tert-butyl hydroperoxide (Sigma-Aldrich, St. Louis, MO) as positive control. Medium was aspirated after each treatment and cells washed with Hank's Balanced Salt Solution (HBSS) from Gibco Life Tech (Carlsbad, CA), at 37 ºC. Subsequently, cells were incubated with 5 μM DCFH-DA (45 min, at 37 ºC and 5 % CO_2, in the dark). Cells were then washed with warm HBSS, and fluorescence (excitation 485 nm, emission 530 nm) was recorded immediately. Three independent assays were performed ($n = 3$), each with three technical replicates.

2.4. Comet assay

The alkaline Comet assay was performed in mini-gel version as described (di Bucchianico et al., 2017). Cells were seeded in 24-well plates (6×10^4 cells/mL) 24 h before exposure. Cells were exposed for up to 48 h and including 25 μM hydrogen peroxide (5 min on ice) as positive control. After exposure, the medium was aspirated, and cells washed twice with warm phosphate-buffered saline (PBS). Cells were then trypsinized and centrifuged, after which the supernatant was discarded, and the pellet resuspended in PBS and placed on ice. Cells were embedded in 0.75 % m/V type VII, low gelling temperature agarose (Sigma-Aldrich A-4018) and placed on a microscopy slide previously coated with 0.3 % agarose (two mini-gels per slide). Two technical replicates were performed per each treatment, with three independent experimental replicates ($n = 3$). After solidification on ice, slides were placed in cold lysis buffer (pH 10, 1 % Triton X-100, 2.5 M NaCl, 10 mM Tris, 0.1 M EDTA) for 60 min, followed by 40 min in cold alkaline buffer (pH 13, 0.3 M NaOH, 1 mM EDTA), both in the dark. Electrophoresis was run at 1.15 V/cm (29 V) in the same alkaline buffer for 30 min, in cold and dark conditions. Slides were then neutralized in 0.4 M Tris pH 7.8 (5 min + 5 min) and washed twice for 5 min in dH2O. Slides were allowed to dry in the dark and then fixed for 5 min in methanol for archiving. Slides were stained for 15 min in cold SYBR green (Life Technologies) diluted in TAE (tris-acetate-EDTA) buffer (1:10,000). One-hundred nucleoids per experimental replica were scored under a DMLB model epifluorescence microscope (Leica Microsystems, Wetzlar, Germany) using the Comet assay IV software (Perspective Instruments, Suffolk, UK).

2.5. In-cell western assay

The In-Cell Western assay was performed to assess levels of γH2AX protein as previously described (de Oliveira Galvão et al., 2022). In brief, 1×10^5 cells/mL were seeded in black and clear bottom 96-well plates for 24 h. Exposure to camptothecin (10 μM) for 1 h was used as positive control. Exposed cells were repeatedly washed with PBS between fixation with 3.7 % formaldehyde and permeabilization with 0.3 % Triton-X, and finally blocked with Intercept® Blocking Buffer (LI-COR Biosciences, USA) supplemented with phosphatase inhibitor (PhosSTOP™ EasyPack, Roche). Cells were incubated with primary antibodies against H2AX phosphorylated at Ser-139 (#9718, Cell Signaling Technology) followed by IRDye® 800CW Goat anti-Rabbit IgG. CellTag™ 700 Stain (LI-COR Biosciences, USA) was used to normalize for cell numbers and all the values were subtracted by the background control (cells + secondary antibody). Fluorescence was detected by the LI-COR Odyssey ® CLx Infrared Imaging System (LI-COR Biosciences, USA).

2.6. Flow cytometric MN assay

The induction of MN was evaluated by flow cytometry using the *In Vitro* Microflow Kit (Litron Laboratories, Rochester, NY) following manufacturer's instructions and previous adaptations (Le Bihanic et al., 2016; McCarrick et al., 2019). In brief, cells were seeded in 96-well plate (2.5×10^4 cells/mL) for 24 h and exposed to the chemicals including a positive control (etoposide, 0.2 μg/mL) in three independent experiments ($n = 3$). After 72 h of exposure, medium was aspirated, and cells were incubated with ethidium monoazide on ice for 30 min under cold white light to allow stain photoactivation. Subsequently, cells were lysed and stained with SYTOX® Green nucleic acid stain for 1.5 h in the dark at 37 °C. Samples were analyzed using a Accuri C6 flow cytometer (BD Bioscience, Franklin Lakes, NJ) with flow set to 30 μL/min, run limit to 175 μL and 10,000 gated nuclei events per sample. Each well was manually resuspended before acquisition to avoid sedimentation.

2.7. CYP1 activity assay

CYP1-dependent ethoxyresorufin-O-deethylase (EROD) activity was measured in cells as previously described (Wincent et al., 2016). In brief, 1×10^5 cells/mL were seeded in 96-well plates for 24 h. Exposure to 2,3,7,8-Tetrachlorodibenzo-p-dioxin (TCDD, 5 nM) and 3′-methoxy-4′-nitroflavone (MNF, 2.5 μM) were included as positive and negative controls (both from Sigma Aldrich). After exposure, medium was aspirated, and cells were incubated with 2 μM 7-ethoxyresorufin in sodium phosphate buffer (50 mM, pH 8.0) followed by 20 min of incubation at 37 °C. The reaction was terminated by addition of cold fluorescamine solution (0.15 mg/mL in acetonitrile), and the formation of resorufin was measured using an Infinite F 200 PRO plate reader (Tecan, Männedorf, Switzerland) at excitation/emission wavelengths 535/590 nm. Enzymatic activity was normalized for the cellular protein content determined by fluorescamine fluorescence at excitation/emission wavelengths 390/485 nm. Data was expressed as relative EROD activity (pmol resorufin/mg protein) compared to unexposed cells.

2.8. Quantitative real-time PCR

Cells were seeded in 6-well plate (3×10^5 cells/mL) for 24 h and following exposure for up to 24 h, total RNA was extracted using RNeasy Mini kit (Qiagen) according to protocol. Reverse transcription was performed using 1 μg RNA and the High Capacity cDNA RT kit (Applied Biosystems) according to protocol. Quantification of gene expression from three experiments was performed in duplicates using Maxima SYBR Green qPCR kit (Thermo Fisher Scientific) with detection on a QuantStudio 5 Real-Time PCR system (Applied Biosystems). Relative gene expression was based on the $2^{-\Delta\Delta}$Ct method using GAPDH as housekeeping gene. Following primers were used: *CYP1A1* forward CACCATCCCCCACAGCAC and reverse ACAAAGACACAACGCCCCTT, *CYP1B1* forward AGTGCAGGCAGAATTGGATCA and reverse AGGACATAGGGCAGGTTGGG, *GAPDH* forward ACAGTTGCCATGTAGACC and reverse TTGAGCACAGGGTACTTTA.

2.9. Statistical analysis

The IC_{50} values were estimated by log(inhibitor) vs. normalized response function using GraphPad Prism 9 statistical software (GraphPad Inc., San Diego, CA). The same software was used for statistical analysis of γH2AX, MN, QPCR and EROD data by one-way ANOVA followed by Dunnett's multiple comparison test. All other analyses were computed using R (Ihaka and Gentleman, 1996). After invalidation of normality and homogeneity of variances, determined by Shapiro–Wilk's and Levene's tests, respectively, Kruskal–Wallis ANOVA-by-Ranks *H* followed by Dunn's test was used for multiple comparisons. The significance level α was set at 0.05 for all analyses and the results are expressed as means ± standard error of mean (SEM). For detecting synergistic or antagonistic mixture interactions the Biochemically Intuitive Generalized Loewe Model (BIGL) package (van der Borght et al., 2017) was used followed by meanR/maxR statistical tests, which allow for identification of statistically significant combined effects and their deviation from the null model (additivity). This strategy was applied to data from cytotoxicity, Comet, and ROS assays. For γH2AX, MN and EROD assays, which did not include enough data for applying the BIGL package, Model Deviation Ratios (MDRs) were determined by comparing the observed effect with the expected (Phyu et al., 2011; Trombini et al., 2016). Previous studies have used MDRs > or < 1 as cutoff for non-additive effects, here MDRs above 1.3 were used as indicative of synergism and MDRs below 0.7 for antagonism (Ünlü Endirlik et al., 2023). SEM values for MDRs were calculated based on the distribution of observed and expected ratios from each sample.

3. Results

3.1. Binary mixtures of B[a]P and DFC cause antagonistic effects on cytotoxicity

The IC_{50} for B[*a*]P in HepG2 cells was found to be almost 150-fold lower than for DFC, i.e. 1.95 μM and 290 μM, respectively (Fig. 1A and B). In fact, only concentrations higher than 500 μM DFC caused significant decrease in cell viability, whereas this threshold for B[*a*]P was 1 μM (Dunn's test, $p < 0.05$). Notably, the effects on cell viability were lower than expected when cells were exposed to binary mixtures (Fig. 1C–F). Co-exposing cells to increasing concentrations of B[*a*]P with a set concentration of DFC at either IC_{50} (290 μM) or ⅕ IC_{50} (58 μM) resulted in an apparent IC_{50} for B[*a*]P at 15 and 14 μM, respectively (Fig. 1C and D), approximately 7-fold lower than what was found for exposure to B[*a*]P alone. Similarly, the cytotoxicity was about 3- and 2-fold lower in cells exposed to increasing concentrations of DFC and B[*a*]P at IC_{50} (1.95 μM) and ⅕ IC_{50} (0.39 μM), respectively, compared to DFC alone (Fig. 1E and F). Accordingly, toxicant interaction analyses using BIGL confirmed the antagonistic effects on cytotoxicity (Fig. 2). Antagonism was most obvious in cells exposed to binary mixtures consisting of 10 μM B[*a*]P and IC_{50} or ⅕ IC_{50} of DFC (BIGL, $p < 0.05$). In contrast, a synergistic effect was observed in response to the combination of 1000 μM DFC and B[*a*]P IC_{50} (BIGL, $p = 0.02$). All other mixtures caused additive effects. Based on these results, cells were exposed to mixtures of B[*a*]P and DFC at ⅕ IC_{50} and/or ½ IC_{50} values in the following experiments.

3.2. Additive effects on ROS induction

Intracellular ROS was only moderately increased in response to B[*a*]P, DFC and the three mixtures (Fig. 3A-C). For B[*a*]P and the mixture treatments, levels of ROS were only significantly increased at 6 h and 12 h, up to 1.5-fold comparative to the control (Dunn's test, $p < 0.05$, Fig. 3B-C). The individual DFC exposures only caused significant alterations in ROS levels in cells exposed to ⅕ IC_{50} after 12 h (Dunnett's test, $p < 0.05$, Fig. 3C). In contrast to cytotoxicity, only additive mixture effects were found on intracellular ROS generation (Fig. 3A-C).

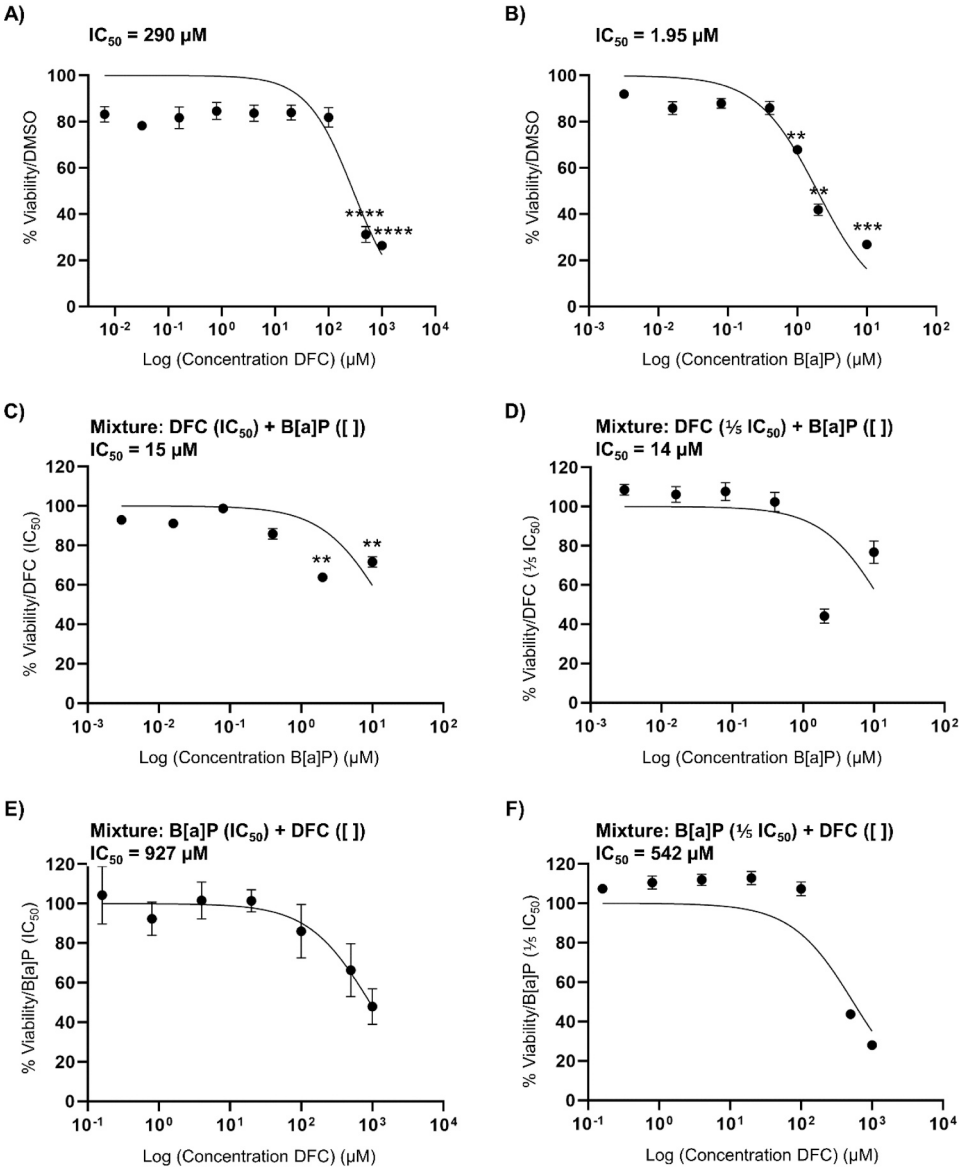

Fig. 1. Assessment of cellular viability at 48 h by Alamar Blue assay. HepG2 cells were exposed to several concentrations of DFC (A), B[*a*]P (B). C - F) Cells were exposed to IC_{50} and ⅕ IC_{50} concentrations of either compound mixed with the full range of concentrations of the other contaminant. Data shows mean ± SEM, $n = 4$, * $p < 0.05$, ** $p < 0.01$, ***$p < 0.001$, **** $p < 0.0001$ as compared with DMSO control through Dunn's test.

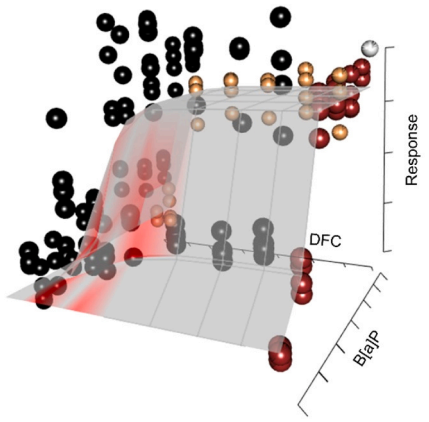

DFC (μM)	B[a]P (μM)	absR	p-value	call
1000	1.95 (IC_{50})	4.532751	0.02	Synergy
290 (IC_{50})	10	4.405321	0.02	Antagonism
500	0.39 (⅕ IC_{50})	4.476373	0.02	Antagonism
58 (⅕ IC_{50})	10	14.34885	0.00	Antagonism

Fig. 2. Interaction analysis of effects from DFC and B[*a*]P mixtures on HepG2 cell viability. Left panel shows surface plot of exposure vs response. Red-colored areas of the surface indicate antagonism. Right panel shows significant non-additive effects based on the Generalized Loewe model followed by meanR/maxR statistic ($p < 0.05$).

3.3. Antagonistic effects on genotoxicity

The possible genotoxic mixture effects of B[*a*]P and DFC in HepG2 cells were assessed by three methods: Comet assay, γH2AX assay and MN assay. Results from the Comet assay showed that induction of DNA strand breaks was more obvious at shorter time points (Fig. 4A, B). In more detail, all exposures except Mixture 2 (½ B[*a*]P IC_{50} + ⅕ DFC IC_{50}), caused significant levels of DNA damage compared to control at 6 h (Dunn's test, $p < 0.05$, Fig. 4A). At 24 h, the significant induction of DNA strand breaks was mainly associated with exposure to B[*a*]P alone although DFC and Mixture 1 (⅕ IC_{50} of both B[*a*]P and DFC) also induced DNA strand breaks (Dunn's test, $p < 0.05$, Fig. 4B). None of the exposures significantly induced DNA strand breaks after 48 h of exposure (Fig. 4C). Notably, mixture interaction analyses indicated antagonistic effects on the induction of DNA strand breaks for all exposure times (Fig. 4A-C). However, only Mixture 2 displayed significant antagonistic effects on levels of DNA strand breaks at 24 h (BIGL, $p = 0.04$). In agreement, levels of γH2AX at 24 h were only significantly induced by B[*a*]P and the mixtures (up to 2.4-fold, Dunnett's test, $p < 0.05$), and all three mixtures displayed a MDR ≤ 0.7, indicative of antagonism (Fig. 5).

Induction of MN (Fig. 6) was only assessed for ½ IC_{50} concentrations of both compounds and the results showed that only B[*a*]P and the mixture significantly induced MN compared to control (Dunnett's test, $p < 0.01$). Although only one mixture was tested, the observed genotoxicity was slightly lower than expected based on additivity (MDR = 0.8). Taken together, all three endpoints and especially DNA strand breaks and γH2AX activation indicated antagonistic genotoxic effects of mixtures with B[*a*]P and DFC.

3.4. Involvement of AhR signaling and CYP1 activity

B[*a*]P is a well-established activator of the aryl hydrocarbon receptor (AhR), leading to downstream induction of CYP1 gene expression and increased metabolic activation of B[*a*]P into genotoxic metabolites (Shimada and Fujii-Kuriyama, 2004). To assess the involvement of this pathway in the observed antagonistic genotoxic effects, the CYP1 enzyme activity and *CYP1A1* and *CYP1B1* gene expression levels were measured at 6 h and 24 h. As shown in Fig. 7A and B, it was only B[*a*]P of the two compounds that significantly induced CYP1 activity at both time points, up to 9-fold compared to control (Dunnett's test, $p < 0.05$). All three mixtures caused similar or lower levels of activity induction compared to B[*a*]P alone at both time points, up to 8.4-fold compared to control (Dunnett's test, $p < 0.05$, Fig. 7A and B). For the three mixtures, all MDRs were ≤ 1, and < 0.7 for Mixture 3 at 6 h and Mixture 1 at 24 h, indicating antagonistic effects on CYP1 activity. TCDD strongly induced CYP1 enzyme activity at both time points, which was completely blocked in the presence of MNF (Dunnett's test, $p < 0.05$). Gene expression analyses (Fig. 7C and D) showed that ½ IC_{50} B[*a*]P and Mixture 3 significantly induced expression of both CYP1 genes at 6 h, but only *CYP1A1* at 24 h, up to 40-fold (Dunnett's test, $p < 0.05$). In contrast, ½ IC_{50} of DFC induced neither of the CYPs indicating that any antagonistic interaction effects occur at the protein level.

4. Discussion

Even though B[*a*]P, a well-known carcinogenic model PAH, and the NSAID diclofenac are expected to have different modes-of-action, the underlying metabolic networks may sufficiently overlap to trigger unforeseen interaction effects. Our findings revealed that HepG2 cells respond unpredictably when exposed to binary mixtures of B[*a*]P and DFC, showing antagonistic effects on induction of cytotoxicity and genotoxicity. Although antagonistic effects were predominant in this study, the observed non-additive effects on the time and dose response for several biomarkers can be a significant confounding factor in mixtures evaluation. These results further corroborate the long-foreseen problem of contaminant mixtures in surface waters of industrialized regions compromising risk assessment for humans and wildlife (Cassee et al., 1998).

Our results showed that B[*a*]P was more than 100-fold more cytotoxic than DFC (IC_{50} of 1.95 μM *vs.* 290 μM). This agrees with previous studies performed in hepatocytes: Lim et al. (2015) and Ünlü Endirlik et al. (2023) reported an IC_{50} for B[*a*]P (48 h) of 1.5–2.0 μM in HepG2 cells and Ellepola et al. (2022) reported an IC_{50} for DFC in HepG2 cells (48 h) at > 250 μM. Relatively high IC_{50} for DFC (> 700 μM) were also observed in HepG2 cells at 24 h (Bort et al., 1999; Granitzny et al., 2017; Wu et al., 2016). Notably, the cytotoxicity of combined exposure to B[*a*]P and DFC diverged from simple additive effects and yielded a significant reduction of cytotoxic effects compared to the exposure to individual compounds. In contrast, additive effects were observed on cellular levels of ROS, although B[*a*]P, DFC, and the three mixtures all induced ROS production.

As expected, B[*a*]P was a more potent genotoxicant than DFC. Our findings are accordant with previous works reporting induction of DNA strand breaks and γH2AX formation in HepG2 cells exposed to B[*a*]P from 0.1 μM to 1 μM (Genies et al., 2013; Lim et al., 2015; Park et al., 2006; Stepnik et al., 2015). Our results for B[*a*]P were similarly in agreement for the induction of MN (Shah et al., 2016), which is an important biomarker for chromosomal instability linked to genomic mutation and tumor development (Fenech et al., 2020; Terradas et al., 2010). The potency of B[*a*]P as genotoxicant and mutagen mainly results from the formation of reactive metabolites by CYPs and AKRs resulting in B[*a*]P diol epoxides and quinones, respectively (Penning,

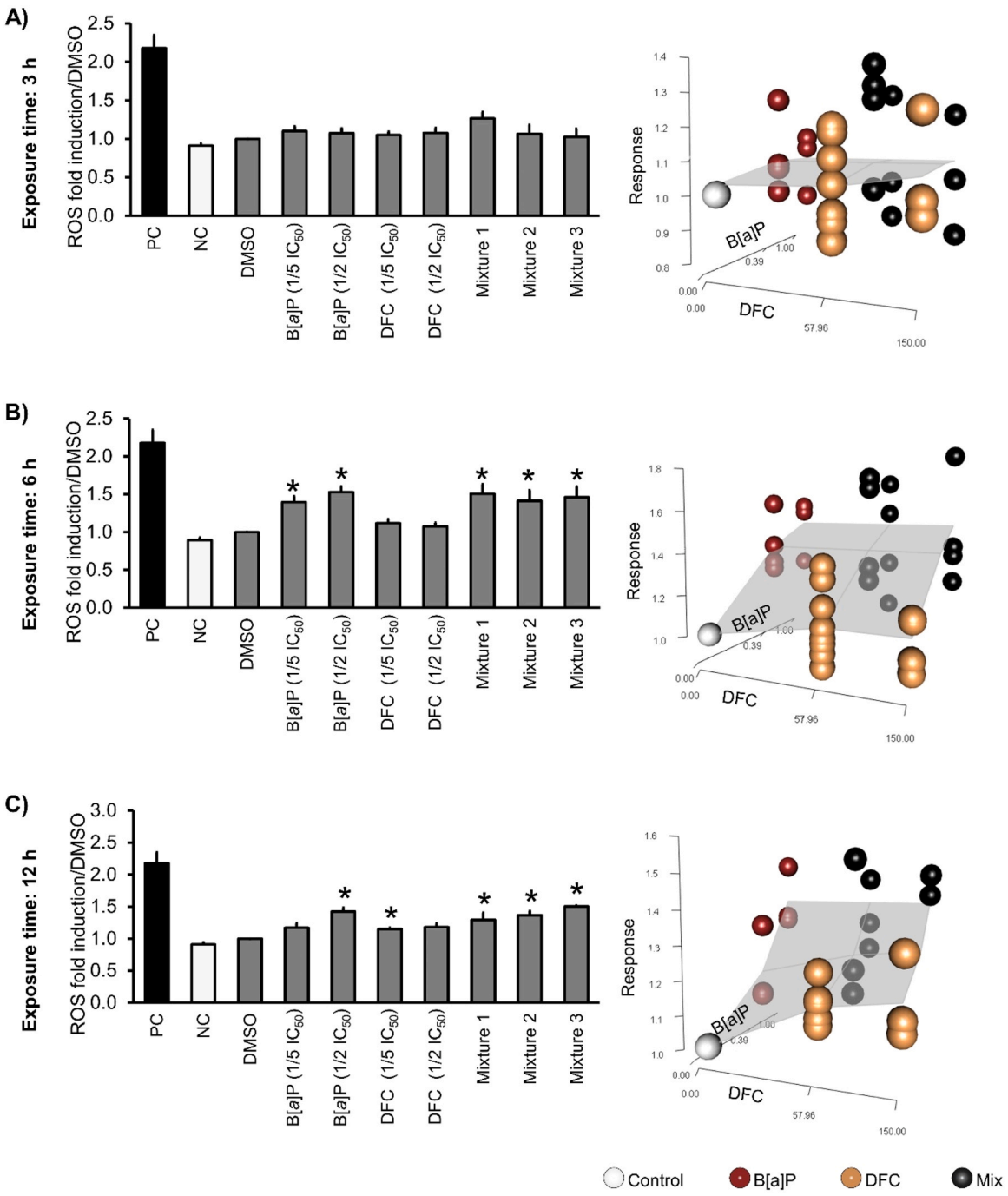

Fig. 3. Assessment of intracellular ROS measured by DCFH-DA assay at (A) 3 h, (B) 6 h and (C) 12 h post exposure. The left panels show relative fold induction of ROS compared to DMSO and right panels show mixture interaction surface plots. HepG2 cells were exposed to individual compounds, Mixture 1: ⅕ IC_{50} of both, Mixture 2: ½ IC_{50} of B[*a*]P and ⅕ IC_{50} of DFC, Mixture 3: ½ IC_{50} of B[*a*]P and ½ IC_{50} of DFC, positive control (PC, 1 mM tert-butyl hydroperoxide). Data shows mean ± SEM, $n = 4$, * $p < 0.05$, as compared with DMSO control through Dunn's test.

2014; Shimada and Fujii-Kuriyama, 2004). While the diol epoxides are responsible for forming bulky DNA adducts, the quinones can redox cycle resulting in ROS formation and oxidative DNA damage. Both routes of metabolism can cause DNA strand breaks that may persist and lead to formation of MN, either as result of replication stress due to replicative blockage by the bulky adduct, or due to extensive oxidative DNA damage due to ROS (Fischer et al., 2018; Penning, 2014). In contrast to B[*a*]P, DFC induced lower levels of genotoxicity. In accordance, several *in vivo* and *in vitro* studies on DFC genotoxicity report the absence of genotoxic effects, as summarized by Hartmann et al. (2021). The low level of genotoxicity may be linked to the suggested mechanism involving the formation of reactive but short-lived acyl glucuronides during phase II metabolism of carboxylic acid drugs like DFC that can damage DNA via glycation or glycoxidation resulting in DNA strand breaks (Grillo et al., 2003; Sallustio et al., 2006). It is not impossible that the induced genotoxicity of DFC observed here could be linked to the formation of these metabolites at early stages of exposure.

Similar to the mixture effects on cytotoxicity, we observed antagonistic mixture effects on all three genotoxicity endpoints investigated here. For all endpoints, this was most clearly observed at higher concentrations and in contrast to the more commonly observed synergistic effects on cytotoxicity and genotoxicity due to secondary toxicity

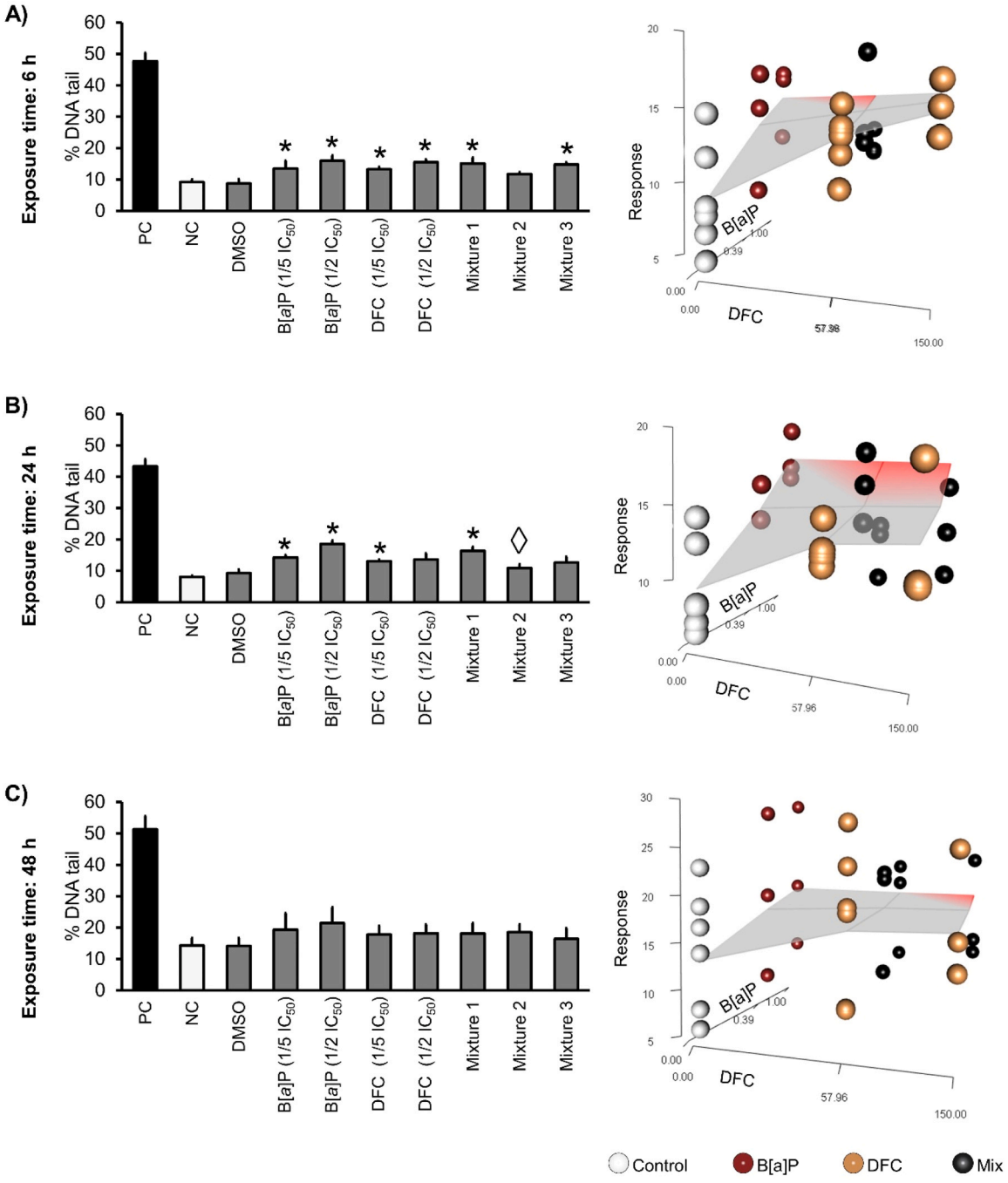

Fig. 4. Assessment of DNA damage in HepG2 cells exposed B[*a*]P, DFC, or their combination determined by the Comet assay after (A) 6 h, (B) 24 h and (C) 48 h of exposure. The left panels show % DNA in tail and right panels the mixture interaction surface plots. HepG2 cells were exposed to individual compounds, Mixture 1: ⅕ IC_{50} of both, Mixture 2: ½ IC_{50} of B[*a*]P and ⅕ IC_{50} of DFC, Mixture 3: ½ IC_{50} of B[*a*]P and ½ IC_{50} of DFC, DMSO, negative control (NC) and positive control (PC, 25 μM hydrogen peroxide). Data shows mean ± SEM, n = 3, * $p < 0.05$ for significant difference as compared with DMSO-control through Dunn's test. ◊ $p = 0.04$ indicate significant antagonistic effects on levels of DNA strand breaks though Generalized Loewe model followed by meanR/maxR statistic (BIGL). Additionally, red colored areas of the surfaces in left 3D graphics suggest antagonistic interactions.

mechanisms activated at elevated concentrations (Boobis et al., 2011). Antagonistic genotoxic effects have been reported previously in mammalian and non-mammalian test models exposed to binary mixtures of various chemicals, including mice (El-Habit and Abdel Moneim, 2014), human liver cells (Gábelová et al., 2013), marine fish (Martins et al., 2016) and freshwater crustaceans (Kundi et al., 2016; Russo et al., 2018). Few of these studies have reported the responsible mechanisms, but it seems that saturation of metabolism or of its activation plays an important role in the antagonistic genotoxic effects observed for binary PAHs *in vivo* and *in vitro* (reviewed in Jarvis et al., 2014).

B[*a*]P and DFC are both metabolized into reactive metabolites by CYPs. B[*a*]P is mainly metabolized into reactive metabolites by CYP1A1 or 1B1 (Shimada and Fujii-Kuriyama, 2004) whereas the most reactive DFC metabolites are produced by CYP2C9 and CYP3A4 (Bort et al., 1999; Leemann et al., 1993; Shen et al., 1999). Addition of specific CYP inhibitors block the cytotoxic effects of B[*a*]P and DFC *in vitro*. Inhibition of CYP1A1 significantly reduced both cytotoxicity and genotoxicity of B[*a*]P in mammalian cells (Babich et al., 1988; Shimada and Guengerich,

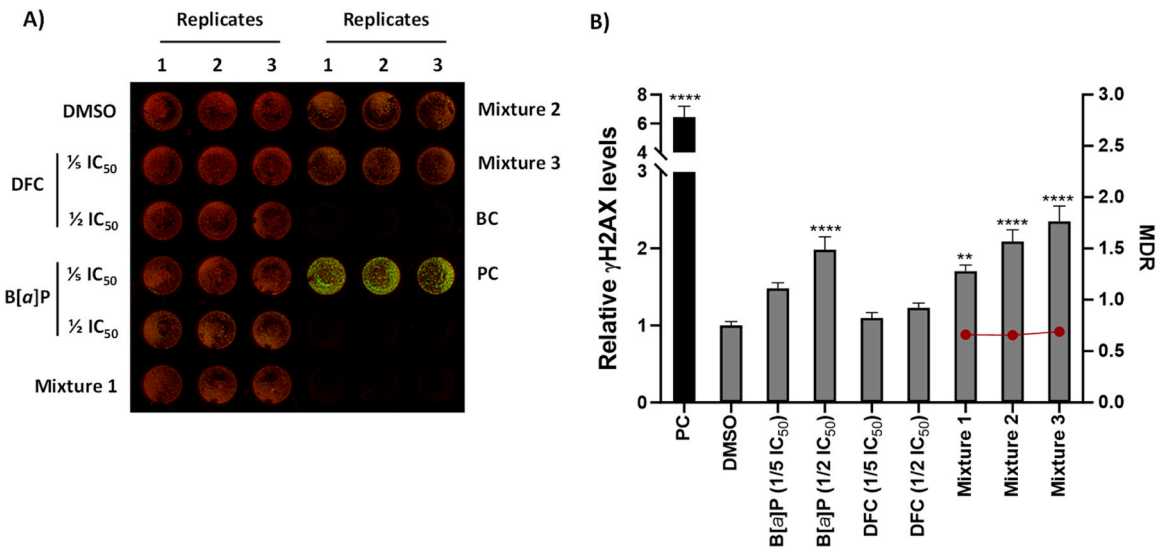

Fig. 5. Assessment of γH2AX activation by ICW at 24 h post exposure. (A) shows representative two-color fluorescence ICW image of γH2AX (green) and CellTag 700 (red). (B) shows relative levels of γH2AX on left y-axis (bars) and MDR on right y-axis (circles). HepG2 cells were exposed to individual compounds, Mixture 1: ⅕ IC_{50} of both, Mixture 2: ½ IC_{50} of B[*a*]P and ⅕ IC_{50} of DFC, Mixture 3: ½ IC_{50} of B[*a*]P and ½ IC_{50} of DFC, positive control (PC, camptothecin, 10 μM). Background (BC, cells + secondary antibody). Data shows mean ± SEM, n = 5, ** $p < 0.01$, **** $p < 0.0001$ as compared with DMSO control through Dunnett's test.

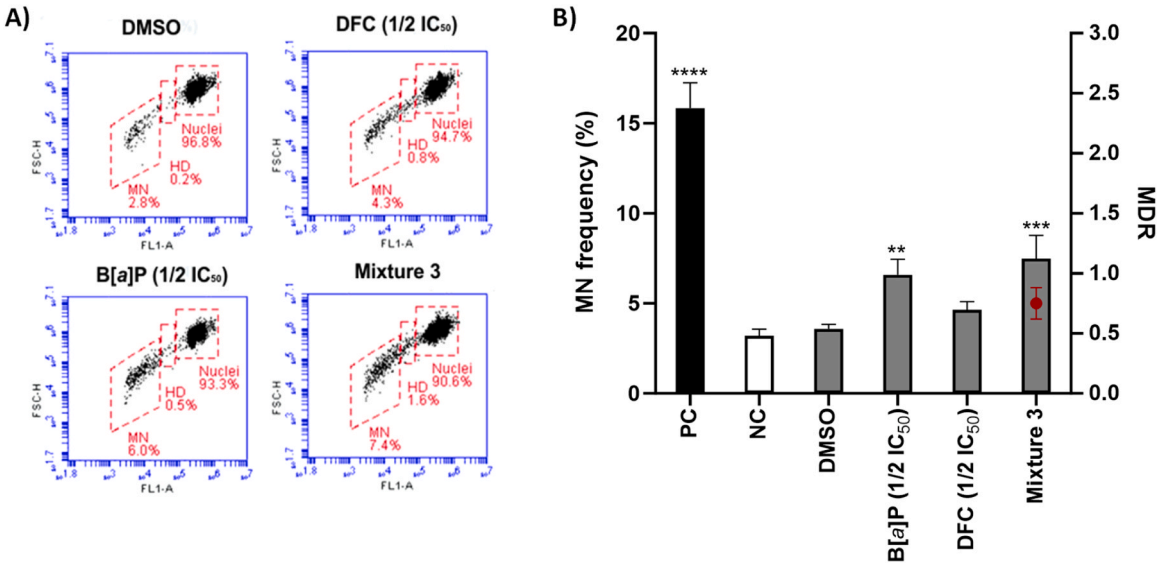

Fig. 6. Assessment of MN frequency by flow cytometry at 72 h post exposure. (A) Representative flow cytometry plots including populations of nuclei, hypodiploid nuclei (HD) and micronuclei (MN). (B) MN frequency in HepG2 cells (left y-axis, bars) and MDR (right y-axis, circle). HepG2 cells were exposed to individual compounds, Mixture 3: ½ IC_{50} of B[*a*]P and ½ IC_{50} of DFC, positive control (PC, etoposide, 0.2 μg/mL). Negative control (NC, only medium). Data is presented as mean ± SEM (n = 8–17). ** $p < 0.01$, ***$p < 0.001$ as compared with DMSO control through Dunnett's test.

2006). Similarly, co-exposure with an inhibitor against CYP2C significantly increased the viability of primary rat hepatocytes and immortalized human HC-04 hepatocytes exposed to DFC (Lauer et al., 2009; Lim et al., 2006). Consequently, interaction effects may occur either due to substrate overlap, induction of CYP gene expression, or enzyme inhibitions. Even though DFC metabolism by CYP1 has not been reported, B[*a*]P can be metabolized into 3-hydroxyl B[*a*]P by CYP2C and CYP3A families (Bauer et al., 1995; Yun et al., 1992). However, basal expression levels and inducibility of these enzymes in HepG2 are low, making this type of substrate overlap unlikely (Westerink and Schoonen, 2007). In addition, our results showed that DFC does not induce CYP1A1 or CYP1B1 gene expression in HepG2 cells and DFC has been shown to only moderately induce CYP1A gene expression in Japanese medaka, Rainbow trout and human hepatocytes (Hong et al., 2007; Lauer et al., 2009; Mehinto et al., 2010). Rather, our results suggest that DFC is a weak CYP1 inhibitor, and that this inhibition was responsible for the reduced levels of genotoxicity due to reduced bioactivation of B[*a*]P, as has been reported previously for mixtures (Jarvis et al., 2014; Shimada and Guengerich, 2006). The few available data on CYP1 inhibition by DFC demonstrates weak to moderate inhibition of CYP1A2 in human liver microsomes (Ohyama et al., 2014; Sanderink et al., 1997) and contradicting results for CYP1A in Rainbow trout liver microsomes and hepatocytes (Burkina et al., 2018; Laville et al., 2004). The exact mechanism by which DFC inhibits CYP1 needs further investigation.

5. Conclusions

The antagonistic effects of co-exposure to B[*a*]P and DFC in HepG2

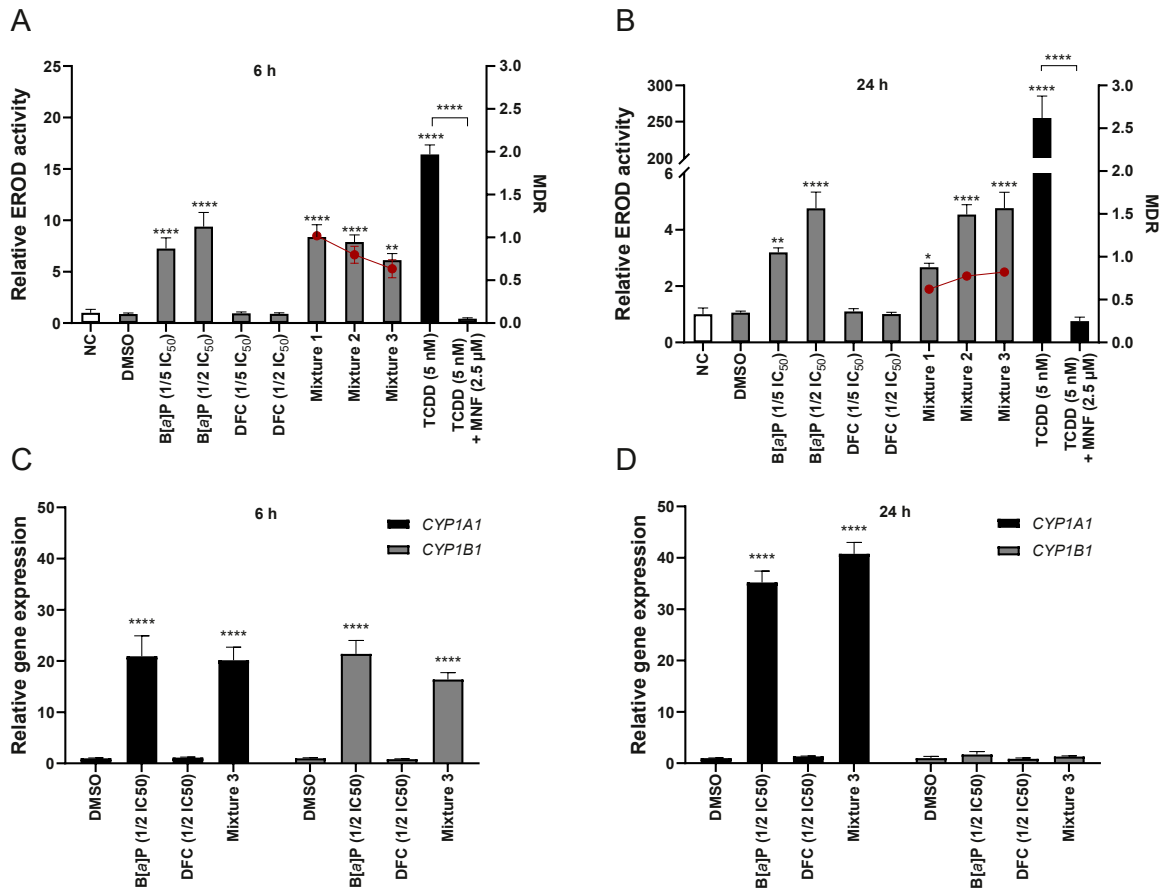

Fig. 7. Assessment of CYP1 EROD activity and gene expression at (A, C) 6 h and (B, D) 24 h post exposure. In panels A and B, eft y-axes show relative EROD activity (bars) and right y-axes MDRs (circles). HepG2 cells were exposed to individual compounds, Mixture 1: ⅕ IC50 of both, Mixture 2: ½ IC50 of B[*a*]P and ⅕ IC50 of DFC, Mixture 3: ½ IC50 of B[*a*]P and ½ IC50 of DFC, TCDD, and TCDD + MNF. Negative control (NC, only medium). Data is presented as mean ± SEM (n = 3–4). *p < 0.05, ** p < 0.01, ***p < 0.001, ****p < 0.0001 as compared with DMSO control or as indicated through Dunnett's test.

cells were observed for cytotoxicity and genotoxicity at concentrations below IC_{50}. Since only minor and additive effects on ROS production were observed, it is unlikely that this mode-of-action contribute to these endpoints. Although the observed antagonistic effects were moderate, our findings demonstrate that exposure to mixed toxicants from different chemical classes with partially overlapping detoxification pathways can lead to unexpected non-additive outcomes, making risk assessment challenging. Questions remain as to whether the same mixing effects would occur at environmental concentrations that are orders of magnitude lower, and how reduced elimination of B[*a*]P due to the presence of DFC would affect aquatic organisms. (Billiard et al., 2006). This issue is also of particular importance when dealing with ubiquitous carcinogens and the growing problem of long-term exposure to pharmaceuticals and their metabolites.

CRediT authorship contribution statement

Pedro M. Costa: Conceptualization, Funding acquisition, Supervision, Writing – original draft. **Marcos Felipe de Oliveira Galvão:** Formal analysis, Investigation, Writing – original draft. **Kristian Dreij:** Conceptualization, Funding acquisition, Supervision, Writing – original draft, Writing – review & editing. **Carla Martins:** Conceptualization, Formal analysis, Investigation, Writing – original draft, Writing – review & editing.

Declaration of Competing Interest

The authors declare that they have no known competing financial interests or personal relationships that could have appeared to influence the work reported in this paper.

Data Availability

Data will be made available on request.

Acknowledgements

The research was funded by Karolinska Institutet. The Portuguese Foundation for Science and Technology (FCT) funded the grant SFRH/BD/120030/2016 to C.M. This work was additionally financed by national funds from FCT in the scope of the projects UIDP/04378/2020 and UIDB/04378/2020 at the Research Unit on Applied Molecular Biosciences (UCIBIO) and the project LA/P/0140/2020 at the Associate Laboratory Institute for Health and Bioeconomy (i4HB).

References

Altenburger, R., Scholz, S., Schmitt-Jansen, M., Busch, W., Escher, B.I., 2012. Mixture toxicity revisited from a toxicogenomic perspective. Environ. Sci. Technol. 46, 2508–2522. https://doi.org/10.1021/es2038036.

Arisan, E.D., Ergül, Z., Bozdağ, G., Rencüzoğulları, Ö., Çoker-Gürkan, A., Obakan-Yerlikaya, P., Coşkun, D., Palavan-Ünsal, N., 2018. Diclofenac induced apoptosis via altering PI3K/Akt/MAPK signaling axis in HCT 116 more efficiently compared to SW480 colon cancer cells. Mol. Biol. Rep. 45, 2175–2184. https://doi.org/10.1007/s11033-018-4378-2.

Babich, H., Sardanaand, M.K., Borenfreund, E., 1988. Acute cytotoxicities of polynuclear aromatic hydrocarbons determined *in vitro* with the human liver tumor cell line, HepG2. Cell Biol. Toxicol. 4, 295–309. https://doi.org/10.1007/BF00058738.

Bauer, E., Zeldin, D., Guo, Z., Ueng, Y.F., Bell, L.C., Guengerich, F.P., 1995. Oxidation of Benzo[a]pyrene by Recombinant Human Cytochrome P450 Enzymes. Chem. Res Toxicol. 8, 136–142. https://doi.org/10.1021/tx00043a018.

Bernanke, J., Köhler, H.-R., 2009. The Impact of Environmental Chemicals on Wildlife Vertebrates. in: Reviews of Environmental Contamination and Toxicology Volume 198. Springer New York, New York, NY, pp. 1–47. https://doi.org/10.1007/978-0-387-09647-6_1.

Beronius, A., Zilliacus, J., Hanberg, A., Luijten, M., van der Voet, H., van Klaveren, J., 2020. Methodology for health risk assessment of combined exposures to multiple chemicals. Food Chem. Toxicol. 143, 111520 https://doi.org/10.1016/j.fct.2020.111520.

le Bihanic, F., di Bucchianico, S., Karlsson, H.L., Dreij, K., 2016. In vivo micronucleus screening in zebrafish by flow cytometry. Mutagenesis 31, 643–653. https://doi.org/10.1093/mutage/gew032.

Billiard, S.M., Timme-Laragy, A.R., Wassenberg, D.M., Cockman, C., Di Giulio, R.T., 2006. The role of the aryl hydrocarbon receptor pathway in mediating synergistic developmental toxicity of polycyclic aromatic hydrocarbons to zebrafish. Toxicol. Sci. 92, 526–536. https://doi.org/10.1093/toxsci/kfl011.

Boelsterli, U.A., 2003. Diclofenac-induced liver injury: a paradigm of idiosyncratic drug toxicity. Toxicol. Appl. Pharm. 192, 307–322. https://doi.org/10.1016/S0041-008X(03)00368-5.

Boobis, A., Budinsky, R., Collie, S., Crofton, K., Embry, M., Felter, S., Hertzberg, R., Kopp, D., Mihlan, G., Mumtaz, M., Price, P., Solomon, K., Teuschler, L., Yang, R., Zaleski, R., 2011. Critical analysis of literature on low-dose synergy for use in screening chemical mixtures for risk assessment. Crit. Rev. Toxicol. https://doi.org/10.3109/10408444.2010.543655.

Bort, R., Ponsoda, X., Jover, R., Gómez-Lechón, M.J., Castell, J.V., 1999. Diclofenac toxicity to hepatocytes: a role for drug metabolism in cell toxicity. J. Pharm. Exp. Ther. 288, 65–72.

Boström, C.E., Gerde, P., Hanberg, A., Jernström, B., Johansson, C., Kyrklund, T., Rannug, A., Törnqvist, M., Victorin, K., Westerholm, R., 2002. Cancer risk assessment, indicators, and guidelines for polycyclic aromatic hydrocarbons in the ambient air. Environ. Health Perspect. 110, 451–488. https://doi.org/10.1289/ehp.110-1241197.

di Bucchianico, S., Cappellini, F., le Bihanic, F., Zhang, Y., Dreij, K., Karlsson, H.L., 2017. Genotoxicity of TiO2 nanoparticles assessed by mini-gel comet assay and micronucleus scoring with flow cytometry. Mutagenesis 32, 127–137. https://doi.org/10.1093/mutage/gew030.

Burkina, V., Sakalli, S., Pilipenko, N., Zlabek, V., Zamaratskaia, G., 2018. Effect of human pharmaceuticals common to aquatic environments on hepatic CYP1A and CYP3A-like activities in rainbow trout (*Oncorhynchus mykiss*): an *in vitro* study. Chemosphere 205, 380–386. https://doi.org/10.1016/j.chemosphere.2018.04.080.

Cassee, F.R., Groten, J.P., Van Bladeren, P.J., Feron, V.J., 1998. Toxicological evaluation and risk assessment of chemical mixtures. Crit. Rev. Toxicol. 28, 73–101. https://doi.org/10.1080/10408449891344164.

Denissenko, M.F., Pao, A., Tang, M.S., Pfeifer, G.P., 1996. Preferential formation of benzo [a]pyrene adducts at lung cancer mutational hotspots in P53. Science 274 (1979), 430–432. https://doi.org/10.1126/science.274.5286.430.

van der Borght, K., Tourny, A., Bagdziunas, R., Thas, O., Nazarov, M., Turner, H., Verbist, B., Ceulemans, H., 2017. BIGL: biochemically intuitive generalized Loewe null model for prediction of the expected combined effect compatible with partial agonism and antagonism. Sci. Rep. 7 (1), 9. https://doi.org/10.1038/s41598-017-18068-5.

Duval, A.P., Troquier, L., Silva, O.D.S., Demartines, N., Dormond, O., 2019. Diclofenac potentiates sorafenib-based treatments of hepatocellular carcinoma by enhancing oxidative stress. Cancers (Basel) 11. https://doi.org/10.3390/cancers11101453.

El-Habit, O.H., Abdel Moneim, A.E., 2014. Testing the genotoxicity, cytotoxicity, and oxidative stress of cadmium and nickel and their additive effect in male mice. Biol. Trace Elem. Res 159, 364–372. https://doi.org/10.1007/s12011-014-0016-6.

Ellepola, N., Viera, T., Patidar, P.L., Rubasinghege, G., 2022. Fate, transformation and toxicological implications of environmental diclofenac: role of mineralogy and solar flux. Ecotoxicol. Environ. Saf. 246 https://doi.org/10.1016/j.ecoenv.2022.114138.

Escher, B.I., Baumgartner, R., Koller, M., Treyer, K., Lienert, J., McArdell, C.S., 2011. Environmental toxicology and risk assessment of pharmaceuticals from hospital wastewater. Water Res 45, 75–92. https://doi.org/10.1016/j.watres.2010.08.019.

Fenech, M., Knasmueller, S., Bolognesi, C., Holland, N., Bonassi, S., Kirsch-Volders, M., 2020. Micronuclei as biomarkers of DNA damage, aneuploidy, inducers of chromosomal hypermutation and as sources of pro-inflammatory DNA in humans. Mutat. Res Rev. Mutat. Res 786, 108342. https://doi.org/10.1016/j.mrrev.2020.108342.

Ferreira, A.L.G., Loureiro, S., Soares, A.M.V.M., 2008. Toxicity prediction of binary combinations of cadmium, carbendazim and low dissolved oxygen on *Daphnia magna*. Aquat. Toxicol. 89, 28–39. https://doi.org/10.1016/j.aquatox.2008.05.012.

Fischer, J.M.F., Zubel, T., Jander, K., Fix, J., Trussina, I.R.E.A., Gebhard, D., Bergemann, J., Bürkle, A., Mangerich, A., 2018. PARP1 protects from benzo[a] pyrene diol epoxide-induced replication stress and mutagenicity. Arch. Toxicol. 92, 1323–1340. https://doi.org/10.1007/s00204-017-2115-6.

Gábelová, A., Poláková, V., Prochazka, G., Kretová, M., Poloncová, K., Regendová, E., Luciaková, K., Segerbäck, D., 2013. Sustained induction of cytochrome P4501A1 in human hepatoma cells by co-exposure to benzo[a]pyrene and 7H-dibenzo[c,g] carbazole underlies the synergistic effects on DNA adduct formation. Toxicol. Appl. Pharm. 271, 1–12. https://doi.org/10.1016/j.taap.2013.04.016.

Gan, T.J., 2010. Diclofenac: An update on its mechanism of action and safety profile. Curr. Med Res Opin. 26, 1715–1731. https://doi.org/10.1185/03007995.2010.486301.

Genies, C., Maître, A., Lefèbvre, E., Jullien, A., Chopard-Lallier, M., Douki, T., 2013. The extreme variety of genotoxic response to benzo[a]pyrene in three different human cell lines from three different organs. PLoS One 8, 1–11. https://doi.org/10.1371/journal.pone.0078356.

Granitzny, A., Knebel, J., Müller, M., Braun, A., Steinberg, P., Dasenbrock, C., Hansen, T., 2017. Evaluation of a human in vitro hepatocyte-NPC co-culture model for the prediction of idiosyncratic drug-induced liver injury: a pilot study. Toxicol. Rep. 4, 89–103. https://doi.org/10.1016/j.toxrep.2017.02.001.

Grillo, M.P., Knutson, C.G., Sanders, P.E., Waldon, D.J., Hua, F., Ware, J.A., 2003. Studies on the chemical reactivity of diclofenac acyl glucuronide with glutathione: identification of diclofenac-S-acyl-glutathione in rat bile. Drug Metab. Dispos. 31, 1327–1336. https://doi.org/10.1124/dmd.31.11.1327.

Harding, S.M., Benci, J.L., Irianto, J., Discher, D.E., Minn, A.J., Greenberg, R.A., 2017. Mitotic progression following DNA damage enables pattern recognition within micronuclei. Nature 548, 466–470. https://doi.org/10.1038/nature23470.

Hartmann, A., Erkman, L., Maremanda, N., Elhajouji, A., Martus, H.J., 2021. Comprehensive review of genotoxicity data for diclofenac. Mutat. Res Genet Toxicol. Environ. Mutagen 866, 503347. https://doi.org/10.1016/j.mrgentox.2021.503347.

Hernández, A.F., Gil, F., Lacasaña, M., 2017. Toxicological interactions of pesticide mixtures: an update. Arch. Toxicol. 91, 3211–3223. https://doi.org/10.1007/s00204-017-2043-5.

Hong, H.N., Kim, H.N., Park, K.S., Lee, S.-K., Gu, M.B., 2007. Analysis of the effects diclofenac has on Japanese medaka (*Oryzias latipes*) using real-time PCR. Chemosphere 67, 2115–2121. https://doi.org/10.1016/j.chemosphere.2006.12.090.

Ihaka, R., Gentleman, R., 1996. R: a language for data analysis and graphics. J. Comput. Graph. Stat. 5, 299–314. https://doi.org/10.1080/10618600.1996.10474713.

Inoue, K., Mizuo, H., Ishida, T., Komori, T., Kusano, K., 2020. Bioactivation of diclofenac in human hepatocytes and the proposed human hepatic proteins modified by reactive metabolites. Xenobiotica 50, 919–928. https://doi.org/10.1080/00498254.2020.1728592.

Inoue, A., Muranaka, S., Fujita, H., Kanno, T., Tamai, H., Utsumi, K., 2004. Molecular mechanism of diclofenac-induced apoptosis of promyelocytic leukemia: dependency on reactive oxygen species, Akt, Bid, cytochrome c, and caspase pathway. Free Radic. Biol. Med 37, 1290–1299. https://doi.org/10.1016/j.freeradbiomed.2004.07.003.

Jarvis, I.W.H., Dreij, K., Mattsson, Å., Jernström, B., Stenius, U., 2014. Interactions between polycyclic aromatic hydrocarbons in complex mixtures and implications for cancer risk assessment. Toxicology 321, 27–39. https://doi.org/10.1016/j.tox.2014.03.012.

Jung, S.H., Lee, W., Park, S.H., Lee, K.Y., Choi, Y.J., Choi, S., Kang, D., Kim, S., Chang, T. S., Hong, S.S., Lee, B.H., 2020. Diclofenac impairs autophagic flux via oxidative stress and lysosomal dysfunction: implications for hepatotoxicity. Redox Biol. 37, 101751 https://doi.org/10.1016/j.redox.2020.101751.

Kaur, J., Sanyal, S.N., 2011. Diclofenac, a selective COX-2 inhibitor, inhibits DMH-induced colon tumorigenesis through suppression of MCP-1, MIP-1α and VEGF. Mol. Carcinog. 50, 707–718. https://doi.org/10.1002/mc.20736.

Khan, S., Naushad, Mu, Govarthanan, M., Iqbal, J., Alfadul, S.M., 2022. Emerging contaminants of high concern for the environment: current trends and future research. Environ. Res 207, 112609. https://doi.org/10.1016/j.envres.2021.112609.

Knasmüller, S., Parzefall, W., Sanyal, R., Ecker, S., Schwab, C., Uhl, M., Mersch-Sundermann, V., Williamson, G., Hietsch, G., Langer, T., Darroudi, F., Natarajan, A. T., 1998. Use of metabolically competent human hepatoma cells for the detection of mutagens and antimutagens. Mutat. Res. - Fundam. Mol. Mech. Mutagen. 402, 185–202. https://doi.org/10.1016/S0027-5107(97)00297-2.

Kundi, M., Parrella, A., Lavorgna, M., Criscuolo, E., Russo, C., Isidori, M., 2016. Prediction and assessment of ecogenotoxicity of antineoplastic drugs in binary mixtures. Environ. Sci. Pollut. Res. 23, 14771–14779. https://doi.org/10.1007/s11356-015-4884-x.

Lauer, B., Tuschl, G., Kling, M., Mueller, S.O., 2009. Species-specific toxicity of diclofenac and troglitazone in primary human and rat hepatocytes. Chem. Biol. Inter. 179, 17–24. https://doi.org/10.1016/j.cbi.2008.10.031.

Laville, N., Aït-Aïssa, S., Gomez, E., Casellas, C., Porcher, J.M., 2004. Effects of human pharmaceuticals on cytotoxicity, EROD activity and ROS production in fish hepatocytes. Toxicology 196, 41–55. https://doi.org/10.1016/j.tox.2003.11.002.

Leemann, T., Transon, C., Dayer, P., 1993. Cytochrome P450TB (CYP2C): a major monooxygenase catalyzing diclofenac 4′-hydroxylation in human liver. Life Sci. 52, 29–34. https://doi.org/10.1016/0024-3205(93)90285-B.

Lewandowska, A.M., Rudzki, M., Rudzki, S., Lewandowski, T., Laskowska, B., 2019. Environmental risk factors for cancer - review paper. Ann. Agric. Environ. Med. 26, 1–7. https://doi.org/10.26444/aaem/94299.

Lim, M.S., Lim, P.L.K., Gupta, R., Boelsterli, U.A., 2006. Critical role of free cytosolic calcium, but not uncoupling, in mitochondrial permeability transition and cell death induced by diclofenac oxidative metabolites in immortalized human hepatocytes. Toxicol. Appl. Pharm. 217, 322–331. ⟨https://doi.org/10.1016/j.taap.2006.09.012⟩.

Lim, H., Mattsson, Å., Jarvis, I.W.H., Bergvall, C., Bottai, M., Morales, D.A., Kummrow, F., Umbuzeiro, G.A., Stenius, U., Westerholm, R., Dreij, K., 2015. Detection of benz[j]aceanthrylene in urban air and evaluation of its genotoxic potential. Environ. Sci. Technol. 49, 3101–3109. https://doi.org/10.1021/es505458g.

Martin, O., Scholze, M., Ermler, S., McPhie, J., Bopp, S.K., Kienzler, A., Parissis, N., Kortenkamp, A., 2021. Ten years of research on synergisms and antagonisms in chemical mixtures: a systematic review and quantitative reappraisal of mixture studies. Environ. Int 146, 106206. https://doi.org/10.1016/j.envint.2020.106206.

Martins, M., Ferreira, A.M., Costa, M.H., Costa, P.M., 2016. Comparing the genotoxicity of a potentially carcinogenic and a noncarcinogenic PAH, singly, and in binary combination, on peripheral blood cells of the European sea bass. Environ. Toxicol. 31, 1307–1318. https://doi.org/10.1002/tox.22135.

McCarrick, S., Cunha, V., Zapletal, O., Vondráček, J., Dreij, K., 2019. *In vitro* and *in vivo* genotoxicity of oxygenated polycyclic aromatic hydrocarbons. Environ. Pollut. 246, 678–687. https://doi.org/10.1016/j.envpol.2018.12.092.

Mehinto, A.C., Hill, E.M., Tyler, C.R., 2010. Uptake and biological effects of environmentally relevant concentrations of the nonsteroidal anti-inflammatory pharmaceutical diclofenac in rainbow trout (*Oncorhynchus mykiss*). Environ. Sci. Technol. 44, 2176–2182. https://doi.org/10.1021/es903702.

Nebert, D.W., Roe, A.L., Dieter, M.Z., Solis, W.A., Yang, Y., Dalton, T.P., 2000. Role of the aromatic hydrocarbon receptor and (Ah) gene battery in the oxidative stress response, cell cycle control, and apoptosis. Biochem Pharm. 59, 65–85. https://doi.org/10.1016/S0006-2952(99)00310-X.

Nys, C., Asselman, J., Hochmuth, J.D., Janssen, C.R., Blust, R., Smolders, E., de Schamphelaere, K.A.C., 2015. Mixture toxicity of nickel and zinc to *Daphnia magna* is noninteractive at low effect sizes but becomes synergistic at high effect sizes. Environ. Toxicol. Chem. 34, 1091–1102. https://doi.org/10.1002/etc.2902.

Oaks, J.L., Gilbert, M., Virani, M.Z., Watson, R.T., Meteyer, C.U., Rideout, B.A., Shivaprasad, H.L., Ahmed, S., Chaudhry, M.J.I., Arshad, M., Mahmood, S., Ali, A., Khan, A.A., 2004. Diclofenac residues as the cause of vulture population decline in Pakistan. Nature 427, 630–633. https://doi.org/10.1038/nature02317.

Ohyama, K., Murayama, N., Shimizu, M., Yamazaki, H., 2014. Drug interactions of diclofenac and its oxidative metabolite with human liver microsomal cytochrome P450 1A2-dependent drug oxidation. Xenobiotica 44, 10–16. https://doi.org/10.3109/00498254.2013.806837.

de Oliveira Galvão, M.F., Sadiktsis, I., Marques Pedro, T., Dreij, K., 2022. Determination of whole mixture-based potency factors for cancer risk assessment of complex environmental mixtures by *in vitro* testing of standard reference materials. Environ. Int 166, 107345. https://doi.org/10.1016/j.envint.2022.107345.

Park, S.Y., Lee, S.M., Ye, S.K., Yoon, S.H., Chung, M.H., Choi, J., 2006. Benzo[a]pyrene-induced DNA damage and p53 modulation in human hepatoma HepG2 cells for the identification of potential biomarkers for PAH monitoring and risk assessment. Toxicol. Lett. 167, 27–33. https://doi.org/10.1016/j.toxlet.2006.08.011.

Penning, T.M., 2014. Human Aldo-Keto reductases and the metabolic activation of polycyclic aromatic hydrocarbons. Chem. Res Toxicol. 27, 1901–1917. https://doi.org/10.1021/tx500298n.

Pereira, L.C., de Souza, A.O., Bernardes, M.F.F., Pazin, M., Tasso, M.J., Pereira, P.H., Dorta, D.J., 2015. A perspective on the potential risks of emerging contaminants to human and environmental health. Environ. Sci. Pollut. Res. 22, 13800–13823. https://doi.org/10.1007/s11356-015-4896-6.

Phyu, Y.L., Palmer, C.G., Warne, M.St.J., Hose, G.C., Chapman, J.C., Lim, R.P., 2011. A comparison of mixture toxicity assessment: examining the chronic toxicity of atrazine, permethrin and chlorothalonil in mixtures to *Ceriodaphnia* cf. *dubia*. Chemosphere 85, 1568–1573. https://doi.org/10.1016/j.chemosphere.2011.07.061.

Rampersad, S.N., 2012. Multiple applications of alamar blue as an indicator of metabolic function and cellular health in cell viability bioassays. Sens. (Switz.) 12, 12347–12360. https://doi.org/10.3390/s120912347.

Rehman, M.S.U., Rashid, N., Ashfaq, M., Saif, A., Ahmad, N., Han, J.I., 2015. Global risk of pharmaceutical contamination from highly populated developing countries. Chemosphere 138, 1045–1055. https://doi.org/10.1016/j.chemosphere.2013.02.036.

Ross, J.A., Nesnow, S., 1999. Polycyclic aromatic hydrocarbons: correlations between DNA adducts and *ras* oncogene mutations. Mutat. Res. Fundam. Mol. Mech. Mutagen. 424, 155–166. https://doi.org/10.1016/S0027-5107(99)00016-0.

Russo, C., Kundi, M., Lavorgna, M., Parrella, A., Isidori, M., 2018. Benzalkonium chloride and anticancer drugs in binary mixtures: reproductive toxicity and genotoxicity in the freshwater crustacean *Ceriodaphnia dubia*. Arch. Environ. Contam. Toxicol. 74, 546–556. https://doi.org/10.1007/s00244-017-0473-y.

Sallustio, B.C., DeGraaf, Y.C., Weekley, J.S., Burcham, P.C., 2006. Bioactivation of carboxylic acid compounds by UDP-glucuronosyltransferases to DNA-damaging intermediates: role of glycoxidation and oxidative stress in genotoxicity. Chem. Res Toxicol. 19, 683–691. https://doi.org/10.1021/tx060022k.

Sanderink, G.J., Bournique, B., Stevens, J., Petry, M., Martinet, M., 1997. Involvement of human CYP1A isoenzymes in the metabolism and drug interactions of riluzole in vitro. J. Pharm. Exp. Ther. 282, 1465–1472. ⟨https://jpet.aspetjournals.org/content/282/3/1465⟩.

Sathishkumar, P., Meena, R.A.A., Palanisami, T., Ashokkumar, V., Palvannan, T., Gu, F. L., 2020. Occurrence, interactive effects and ecological risk of diclofenac in environmental compartments and biota - a review. Sci. Total Environ. 698, 134057 https://doi.org/10.1016/j.scitotenv.2019.134057.

Selwe, K.P., Thorn, J.P.R., Desrousseaux, A.O.S., Dessent, C.E.H., Sallach, J.B., 2022. Emerging contaminant exposure to aquatic systems in the Southern African development community. Environ. Toxicol. Chem. 41, 382–395. https://doi.org/10.1002/etc.5284.

Shah, U.K., Seager, A.L., Fowler, P., Doak, S.H., Johnson, G.E., Scott, S.J., Scott, A.D., Jenkins, G.J.S., 2016. A comparison of the genotoxicity of benzo[a]pyrene in four cell lines with differing metabolic capacity. Mutat. Res Genet Toxicol. Environ. Mutagen 808, 8–19. https://doi.org/10.1016/j.mrgentox.2016.06.009.

Shen, S., Marchick, M.R., Davis, M.R., Doss, G.A., Pohl, L.R., 1999. Metabolic activation of diclofenac by human cytochrome P450 3A4: Role of 5-hydroxydiclofenac. Chem. Res Toxicol. 12, 214–222. https://doi.org/10.1021/tx9802365.

Shimada, T., 2006. Xenobiotic-metabolizing enzymes involved in activation and detoxification of carcinogenic polycyclic aromatic hydrocarbons. Drug Metab. Pharm. 21, 257–276. https://doi.org/10.2133/dmpk.21.257.

Shimada, T., Fujii-Kuriyama, Y., 2004. Metabolic activation of polycyclic aromatic hydrocarbons to carcinogens by cytochromes P450 1A1 and 1B1. Cancer Sci. https://doi.org/10.1111/j.1349-7006.2004.tb03162.x.

Shimada, T., Guengerich, F.P., 2006. Inhibition of human cytochrome P450 1A1-, 1A2-, and 1B1-Mediated activation of procarcinogens to genotoxic metabolites by polycyclic aromatic hydrocarbons. Chem. Res Toxicol. 19, 288–294. https://doi.org/10.1021/tx050291v.

Silins, I., Högberg, J., 2011. Combined toxic exposures and human health: biomarkers of exposure and effect. Int J. Environ. Res Public Health 8, 629–647. https://doi.org/10.3390/ijerph8030629.

Škrbić, B.D., Kadokami, K., Antić, I., 2018. Survey on the micro-pollutants presence in surface water system of northern Serbia and environmental and health risk assessment. Environ. Res. 166, 130–140. https://doi.org/10.1016/j.envres.2018.05.034.

Stepnik, M., Spryszyńska, S., Smok-Pieniazek, A., Ferlińska, M., Roszak, J., Nocuń, M., 2015. The modulating effect of ATM, ATR, DNA-PK inhibitors on the cytotoxicity and genotoxicity of benzo[a]pyrene in human hepatocellular cancer cell line HepG2. Environ. Toxicol. Pharm. 40, 988–996. https://doi.org/10.1016/j.etap.2015.10.010.

Ternes, T.A., 1998. Occurrence of drugs in German sewage treatment plants and rivers. Water Res. 32, 3245–3260. https://doi.org/10.1016/S0043-1354(98)00099-2.

Terradas, M., Martín, M., Tusell, L., Genescà, A., 2010. Genetic activities in micronuclei: is the DNA entrapped in micronuclei lost for the cell? Mutat. Res Rev. Mutat. Res. 705, 60–67. https://doi.org/10.1016/j.mrrev.2010.03.004.

Trombini, C., Hampel, M., Blasco, J., 2016. Evaluation of acute effects of four pharmaceuticals and their mixtures on the copepod *Tisbe battagliai*. Chemosphere 155, 319–328. https://doi.org/10.1016/j.chemosphere.2016.04.058.

Ünlü Endirlik, B., Wincent, E., Dreij, K., 2023. Non-additive mixture effects of benzo[a]pyrene and pesticides *in vitro* and *in vivo*: Role of AhR signaling. Environ. Pollut. 316, 120510 https://doi.org/10.1016/j.envpol.2022.120510.

Verlicchi, P., al Aukidy, M., Zambello, E., 2012. Occurrence of pharmaceutical compounds in urban wastewater: Removal, mass load and environmental risk after a secondary treatment-a review. Sci. Total Environ. 429, 123–155. https://doi.org/10.1016/j.scitotenv.2012.04.028.

Vystavna, Y., Frkova, Z., Celle-Jeanton, H., Diadin, D., Huneau, F., Steinmann, M., Crini, N., Loup, C., 2018. Priority substances and emerging pollutants in urban rivers in Ukraine: occurrence, fluxes and loading to transboundary European Union watersheds. Sci. Total Environ. 637–638 1358–1362. https://doi.org/10.1016/j.scitotenv.2018.05.095.

Wagner, N.D., Simpson, A.J., Simpson, M.J., 2018. Sublethal metabolic responses to contaminant mixture toxicity in *Daphnia magna*. Environ. Toxicol. Chem. 37 (9), 2448–2457. https://doi.org/10.1002/etc.4208.

Wang, H., Joseph, J.A., 1999. Quantifying cellular oxidative stress by. Free Radic. Biol. Med 27, 612–616.

Westerink, W.M.A., Schoonen, W.G.E.J., 2007. Cytochrome P450 enzyme levels in HepG2 cells and cryopreserved primary human hepatocytes and their induction in HepG2 cells. Toxicol. Vitr. 21, 1581–1591. https://doi.org/10.1016/j.tiv.2007.05.014.

WHO, 2021. Human Health Effects of Polycyclic Aromatic Hydrocarbons as Ambient Air Pollutants Report of the Working Group on Polycyclic Aromatic Hydrocarbons of the Joint Task Force on the Health Aspects of Air Pollution.

Wincent, E., Le Bihanic, F., Dreij, K., 2016. Induction and inhibition of human cytochrome P4501 by oxygenated polycyclic aromatic hydrocarbons. Toxicol. Res. 5, 788–799. https://doi.org/10.1039/C6TX00004E.

Wogan, G.N., Hecht, S.S., Felton, J.S., Conney, A.H., Loeb, L.A., 2004. Environmental and chemical carcinogenesis. Semin Cancer Biol. 14, 473–486. https://doi.org/10.1016/j.semcancer.2004.06.010.

Wu, Y., Geng, X. chao, Wang, J. feng, Miao, Y. fa, Lu, Y., li, Li, B., 2016. The HepaRG cell line, a superior in vitro model to L-02, HepG2 and hiHeps cell lines for assessing drug-induced liver injury. Cell Biol. Toxicol. 32, 37–59. https://doi.org/10.1007/s10565-016-9316-2.

Yu, Y., Wang, Z., Yao, B., Zhou, Y., 2024. Occurrence, bioaccumulation, fate, and risk assessment of emerging pollutants in aquatic environments: a review. Sci. Total Environ. 923, 171388 https://doi.org/10.1016/j.scitotenv.2024.171388.

Yun, C.-H., Shimada, T., Guengerich, F.P., 1992. Roles of HUman Liver Cytochrome P4502C and 3A enzymes in the 3-Hydroxylation of Benzo(a)pyrene. Cancer Res 52, 1868–1874.